Wrench Faulting and Trap Breaching: A Case Study of the Kizler North Field, Lyon County, Kansas, USA

Md Nahidul Hasan*[1,2], Sally Potter-McIntyre[2], Steve Tedesco[3]
1 Department of Earth and Atmospheric Sciences, University of Houston, Texas, USA
2 Department of Geology, Southern Illinois University, Carbondale, Illinois, USA
3 Running Foxes Petroleum Inc., Centennial, Colorado, USA
Correspondence: nahidju13@gmail.com; mhasan11@uh.edu

The Kizler North Field in northwest Lyon County, Kansas, is a producing field with structures associated with both uplift of the Ancestral Rockies (Pennsylvanian to early Permian) and reactivation of structures along the Proterozoic midcontinent rift system (MRS), which contributed to the current complex and poorly understood play mechanisms. The Lower Paleozoic dolomitic Simpson Group, Viola Limestone, and "Hunton Group" are the reservoir units within the field. These units have significant vuggy porosity, which is excellent for field potential; however, in places, the reservoir is inhibited by high water saturation. The seismic data show that two late-stage wrench fault events reactivated existing faults. The observed wrench faults exhibit secondary P, R', and R Riedel shears, which likely resulted from Central Kansas uplift-MRS wrenching. The latest stage event breached reservoir caprock units during post-Mississippian to pre-Desmoinesian time and allowed for hydrocarbon migration out of the reservoirs. Future exploration models of the Kizler North and analog fields should be based on four play concepts: 1) four-way closure with wrench-fault-related traps, 2) structural highs in the Simpson Group and Viola Limestone, 3) thick "Hunton Group," and 4) presence of a wrench fault adjacent to the well location that generates subtle closure but not directly beneath it, which causes migration out of reservoirs. In settings where complex structural styles are overprinted, particular attention should be paid to the timing of events that may cause breaches of seals in some structures but not others. Mapping the precise location and vertical throw of the reactivated wrench faults using high-resolution seismic data can help reduce the drilling risk in analog systems.

INTRODUCTION

Kizler North Field is located in the Forest City basin in the midcontinent of North America (fig. 1). The field produced ~35,000 bbls of oil from 1972 to 2020 (KGS oil and gas wells database, 2020). The majority of production is from the Silurian-Devonian "Hunton Group," and the source rock is within the lower portion of the Ordovician Simpson Group. Geographically, the Kizler North Field is in the northwestern part of Lyon County, Kansas (figs. 1, 2). The field is near the western flank of the Forest City basin and on the northern flank of the Bourbon arch (O'Connor, 1953).

The main subsurface structures in the study area are Precambrian faults that were reactivated during the Phanerozoic. These faults control tectonic expression within the Kizler North Field. Until recently, the structural pattern and migration pathways of this field were poorly defined owing to the subtlety of the reactivated faults (Carlson, 1999; Hasan, 2019). New exploration models are needed to discover the remaining petroleum potential in this area

Midcontinent Geoscience is an open-access, peer-reviewed journal of the Kansas Geological Survey. The journal publishes original research on a broad array of geoscience topics, with an emphasis on the midcontinent region of the United States, including the Great Plains and Central Lowland provinces.

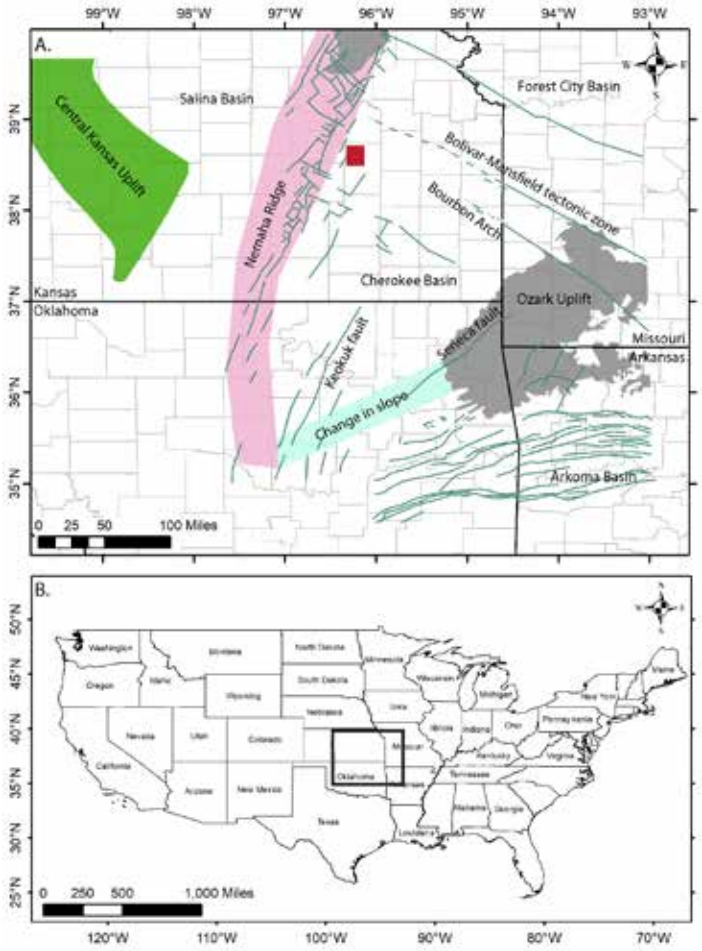

Figure 1. (a) Regional framework showing principal structural features of Kansas and the surrounding region using colored polygons with documented fault systems. The red box shows the approximate location of the study area (modified from Tedesco, 2015; Merriam and Goebel, 1956; and Baker, 1962). Major structural features include the Nemaha ridge (pink) and the Central Kansas uplift (green). (b) Location of the study area.

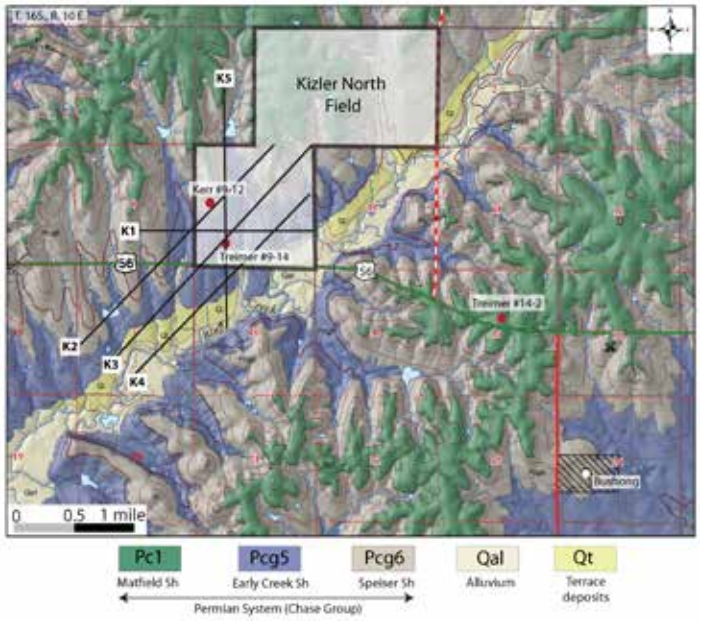

Figure 2. Geologic map of the study area showing exposed unit boundaries at present day. The black outlined polygons show the Kizler North Field's location. Red dots represent the location of the wells used for petrophysical interpretation. The white circle represents the location of Bushong, the nearest town (modified from KGS oil and gas wells database, 2020).

and for the characterization of similar underexplored reservoirs. This research article aims to integrate geological, geophysical, and petrophysical interpretations to better understand the future play concepts for this field and its analog fields.

REGIONAL GEOLOGY AND STRATIGRAPHY

The Forest City basin (fig. 1) was initially a structural and topographic post-Mississippian basin that developed when the formation of the Nemaha anticline divided the North Kansas basin into the Salina basin and Forest City basin (Lee, 1943; Merriam, 1963, 2010). During the Pennsylvanian, sediments were deposited in marine and deltaic environments, with the thickest accumulations in the deepest part of this basin (Lee, 1943; Merriam, 2010). The extent and thickness of these deposits define the extent and depth of the basin (Lee, 1943; Merriam, 2010).

The Phanerozoic tectonic pattern that controls sedimentation and diagenesis in Kansas is a direct reflection of its Precambrian history, and many cratonic structures are simply rejuvenation of pre-Phanerozoic weakness planes (Carlson, 1999; Gerhard, 2004). During the latest Archean or early Proterozoic, the crystalline basement of the midcontinent of North America experienced north-south compressional strain and the resultant wrench faulting formed orthogonal crustal blocks with northeast- and northwest-oriented faults (Sims, 1990; Baars, 1995). The compressional stress field began to relax by 1.2 Ga, and extension and volcanic activity along the midcontinent rift system (MRS) slowly worked southward from the Canadian Shield, ending in Kansas in the latest Proterozoic time (Baars, 1995). Cooling and deformation of the rift by 1.2 Ga permitted fractures and faults to develop (Van Schmus et al., 1993).

During the early Paleozoic, another structure trending N45°W across central Kansas, referred to as the ancestral Central Kansas uplift, developed in relationship to pre-existing structures that were likely established during the accretionary history of the midcontinent (Berendson and Blair, 1986). The exposed rocks were subjected to erosion for such a long period that the surface was worn down

nearly to sea level (Lee, 1943; Merriam, 2010). By Late Mississippian time, the region was again uplifted by gentle folding (Ouachita Orogeny; Berendsen and Blair, 1986) that acted as a precursor to two principal folds that developed in conjunction with the Forest City basin: 1) the Nemaha ridge (N20°E), which is a major post-Mississippian to pre-Desmoinesian structure (Merriam, 2010; Burberry et al., 2015), and 2) its contemporaneous counterpart, the Central Kansas uplift (CKU), which exploited its ancestral trend (Merriam, 1963, 2010). The crest of the Nemaha ridge then underwent further erosion prior to the advancement of the sea over the area and deposition of Pennsylvanian strata (Lee, 1943).

Reservoir units are the Simpson Group and Viola Limestone of Ordovician age and the Late Devonian "Hunton Group" (O'Connor, 1953; Merriam, 2010) (fig. 3). The lithology of the Simpson Group, Viola Limestone, and "Hunton Group" in the Kizler North Field is dominantly dolomite. All three of these reservoir units have excellent porosity (approximately 10–12% effective porosity; Jensik, 2013). Low-temperature hydrothermal fluid migration through the open wrench fault/fracture system caused dolomitization and likely resulted in the enhancement of effective porosity in the reservoir (Tedesco, 2017). According to Gerhard (2004), such low-temperature hydrothermal fluids were probably expelled by tectonic compression during the Ouachita-Marathon Orogeny (Ordovician through Pennsylvanian) from the Anadarko and Arkoma basins. The diagenesis and dolomitization by low-temperature hydrothermal fluid controlled the dolomite crystal size (0.0125 mm to 3.5 mm) and crystal fabric, ultimately influencing the effective porosity and permeability of the Paleozoic reservoir rocks in Kansas (Jensik, 2013; Tedesco, 2017). The vuggy porosity in the reservoir rocks of the Kizler North Field typically has a pore diameter greater than 1/16 mm and is not fabric selective (Choquette and Pray, 1970). The source rock for the system (i.e., the lower part of the Ordovician Simpson Group) has total organic content (TOC) greater than 1.1 wt% and contains Type I and II kerogen (Jensik, 2013).

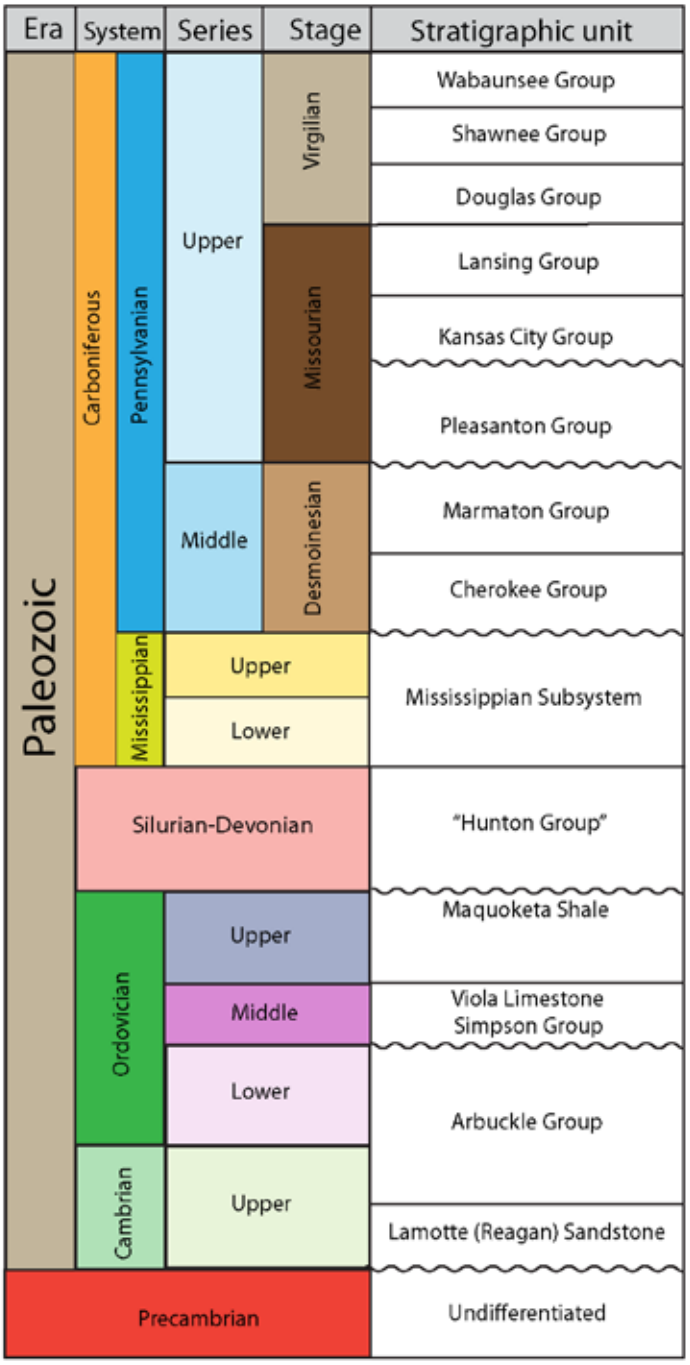

Figure 3. Stratigraphic column summarizing the major lithostratigraphic units of Kansas (modified from Cansler and Carr, 2001; Zeller, 1968).

DATASET AND METHODOLOGY

Potential fields data

We used gravity and aeromagnetic data to understand the structural configuration of the basement of the study area. First, gravity and magnetic data were interpreted through a qualitative review of color-shaded relief of total magnetic intensity, reduced to the pole transform maps, and Bouguer gravity maps. A quantitative analysis of the aeromagnetic data was incorporated to understand the depth to source. This interpretation used 2-D Werner deconvolution-based algorithms as a basis for the interactive analyses of the depth to and horizontal position of source bodies and the related parameters of dip and susceptibility (Werner, 1953; Ku and Sharp, 1983). The method is an iterative, two-dimensional inversion technique that eliminates interference from adjoining,

often overprinted, anomalies. The Werner calculations provide clusters of solutions that can be interpreted as the top of the basement and can yield relatively accurate results if constrained through other data types (e.g., seismic, well data).

Seismic interpretation

We used five 2-D seismic lines with a frequency range of 10–110 Hz and 24-fold data. Stratigraphic tops were correlated to seismic horizons for the major identifiable units using synthetic seismograms generated from sonic and density logs (fig. 4). We used statistical extracted wavelets from the intersecting seismic lines to generate the synthetic seismograms as described in Onajite (2014). Stratigraphic tops of the wells were correlated to seismic horizon for the major identifiable units, and a reasonably good fit was observed with bulk shifting of only 4 milliseconds (ms). Time structure maps and isochron maps were generated after picking horizons and fault mapping. The time structure maps were created using a 1 ms contour interval. Time structure and isochron maps show two-way travel time (TWTT) to the picked horizon. In this research, time structure and isochron maps were not converted into depth because check-shot or vertical sounding profile (VSP) data were unavailable for the study area.

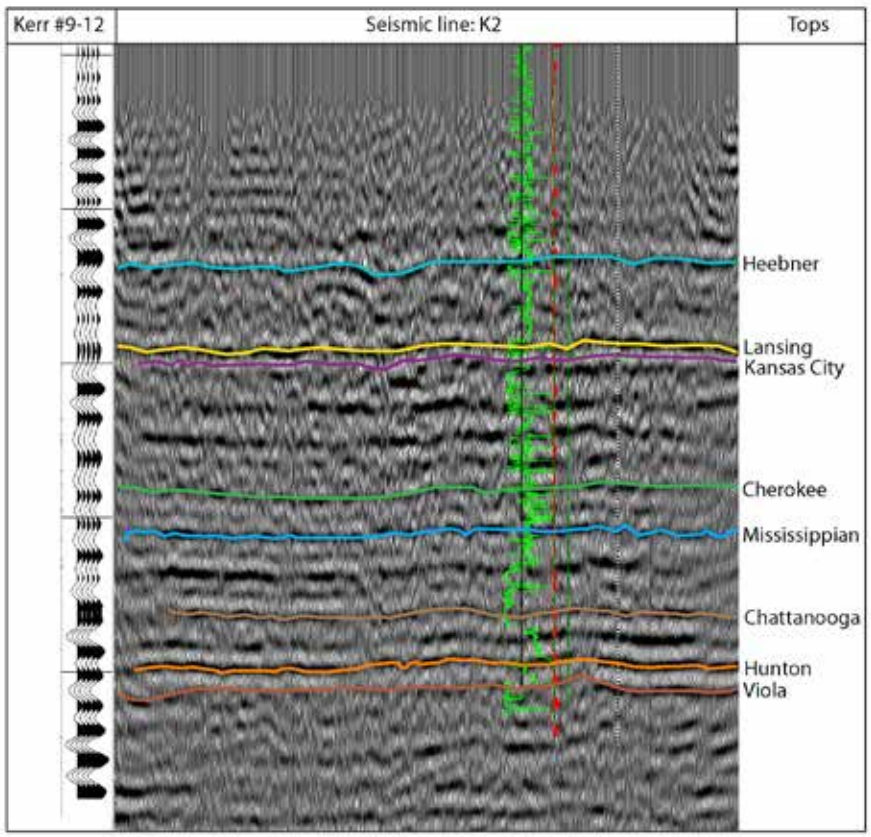

Figure 4. Well-to-seismic tie using synthetic seismograms shows a good match. Synthetic seismograms were generated using density (green curve) and sonic log for the Kerr #9-12 well. Calculated synthetic reflections and correlated stratigraphic tops are shown.

Petrophysical interpretation

Using petrophysical data, attributes of the producing units were determined. To provide robust petrophysical analysis, this study incorporates log mnemonic standardization, depth shifting, and data-conditioning techniques to organize, examine, and in some cases rectify raw well-log data. All well logs in this study were depth shifted to the gamma-ray log. Unit tops were determined by comparing gamma-ray fluctuations with known lithologies from mud logging (table 1).

Well logs of three wells (Treimer #9-14, Kerr #9-12, and Treimer #14-2) were used to evaluate and analyze the petrophysical properties of the volume of clay (VDCL), water saturation (Sw), oil saturation (So), total porosity (PHIT), and water resistivity (Rw). The "Hunton Group," Viola Limestone, and Simpson Group were analyzed for these parameters because these three units are the only reported producing reservoirs in nearby fields (KGS oil and gas wells database, 2020). Gamma-ray, neutron, and density logs were selected as the input curves for calculating the clay volume. The gamma-ray cutoffs were determined from the "Hunton Group," and the validity of their baselines was determined by comparing results obtained from neutron-density cross-plots. Mud logging showed negligible clay volume and corroborates the use of gamma-ray logs. A combined clay volume curve (VDCL) is presented in the final plot.

$$VDCL = (GR - GR_{clean}) / (GR_{clay} - GR_{clean}) \quad \text{Eq. 1}$$

where GR = gamma-ray log, GR_{clay} = gamma-ray log in shale zone, and GR_{clean} = gamma-ray log in clean sand zone. The minimum and maximum gamma-ray values were 12 gAPI and 150 gAPI.

Archie's equation was selected for calculating the water saturation in this study. Neutron, density, sonic, deep resistivity, shallow resistivity, clay volume, and temperature

Table 1. Stratigraphic unit tops identified from well logs (collected from KGS oil and gas wells database). The depth values are in feet.

Well Name	API	Field Name	Longitude	Latitude	Total depth	Heebner	Lansing	Kansas City	BKC	Lenapah	Cherokee	Mississippian	Chattanooga
Treimer #14-2	15-111-20482	Kizler North	-96.2697101	38.6634592	3357	1277	1570	1720	1949	2048	2198	2607	2971
Treimer #9-14	15-111-20483	Kizler North	-96.3109452	38.6686189	3263	1155	1436	1580	1811	1918	2068	2460	2806
Kerr #9-12	15-111-20481	Kizler North	-96.3134663	38.6739201	3327	1195	1472	1626	1852	1957	2104	2490	2855

Well Name	API	Field Name	Longitude	Latitude	Total depth	"Hunton"	Maquoketa	Viola	Simpson	St.Peter	Arbuckle	LaMotte	Precambrian
Treimer #14-2	15-111-20482	Kizler North	-96.2697101	38.6634592	3357	3114	3160	3226	3321	3357	---	---	---
Treimer #9-14	15-111-20483	Kizler North	-96.3109452	38.6686189	3263	2950	2982	3050	3142	3170	3218	---	3250
Kerr #9-12	15-111-20481	Kizler North	-96.3134663	38.6739201	3327	3002	3033	3103	3194	3223	3273	3324	---

gradient were chosen as input curves (Archie, 1952). Selected inputs for Archie's cementation exponent (m), saturation exponent (n), and tortuosity component (a) were 1.8, 2, and 1, respectively, because these values are typically used for carbonate rocks (Archie, 1952). The initial porosity model used was a neutron density model. The principal output curves were total porosity (PHIT) and water saturation (Sw). A three-mineral model with dolomite, sand, and clay was used as the main lithology because the "Hunton Group," Viola Limestone, and Simpson Group are primarily dolomitic as described in mud-log reports.

The Archie equation is given below:

$$Sw = ((a*Rw) / (Rt*PHIT^m))^{(1/n)} \quad \text{Eq. 2}$$

where Sw = water saturation, m = cementation exponent, n = saturation exponent, a = tortuosity component, Rw = water resistivity, and PHIT = total porosity

Water resistivity (Rw) for reservoir intervals in the Hunton, Viola, and Simpson groups were 0.18, 0.26, and 0.17, respectively (personal communication, Running Foxes Petroleum Inc.). RHOMA-Umaa mineral composition plots were configured for each of the units to interpret the lithology of the target zones (Hasan, 2019). Figure 5 shows a representative RHOMA-Umaa plot of the "Hunton Group" for the Treimer #9-14 well.

$$Umaa = (RHOB*PE-PHIT*Ufluid) / (1-PHIT) \quad \text{Eq. 3}$$

where Umaa = bulk photoelectric absorption of the mineral matrix, RHOB = bulk density, PE = photoelectric log, Ufluid = photoelectric absorption of drilling fluid, and PHIT = total porosity.

This study identified reservoir and pay zones by assigning cutoff values to the volume of shale (Vsh), effective porosity (PHIE), and water saturation (Sw) parameters (Brooks and Montolvo, 2012) and by calculating curve statistics across each zone of interest. Reservoir flags were assigned to intervals with total porosity values above 10% and clay volumes below 65%. The 50th-percentile (P50) cutoff sensitivity values of PHIT and Vsh were obtained using the Cutoff Sensitivity module in the Interactive Petrophysics software. The mean cutoff (P50) for reservoir zone identification was selected as it incorporates both the optimistic (P90) and the pessimistic (P10) scenario. Pay flags were calculated the same way as reservoir flags. The main difference between reservoir and pay flags is that the static cutoff value assigned to water saturation is also

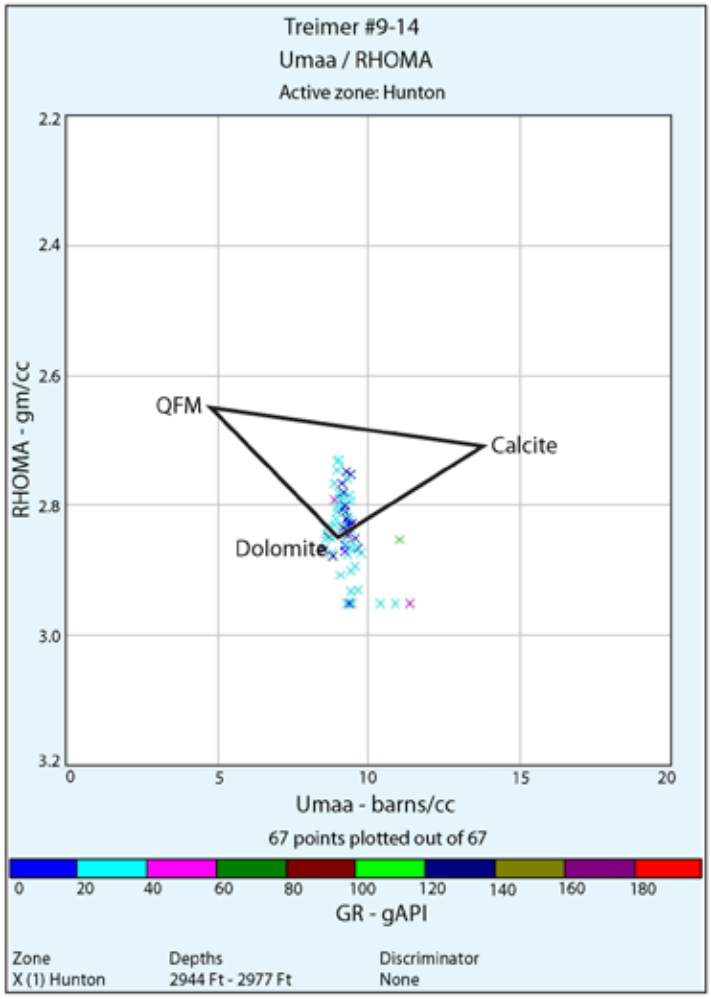

Figure 5. Representative RHOMA-Umaa mineral composition plot of the "Hunton Group" from the Treimer #9-14 well showing a mainly dolomitic reservoir. The colors of the points represent the response from the gamma-ray log.

incorporated to eliminate water-filled reservoirs and highlight hydrocarbon reservoirs (pay zone). Water saturation cutoff values were set to 65%. Oil in place for each reservoir interval was calculated to understand the control of water saturation and gross reservoir volume.

RESULTS

Basement architecture

Using Bouguer gravity, total magnetic intensity (TMI), and reduced to pole transforms (RTP-TMI) of basement anomalies, we found in general that the gravity lineaments appeared to be less pronounced than magnetics. A NNE-SSW magnetic anomaly is readily observable in TMI and RTP-TMI maps (fig. 6a and 6b). In comparison, the Bouguer gravity shows an overall low gravity response rather than individual anomaly trends (fig. 6c). As anomalies are better highlighted in the magnetic maps, the spatial and

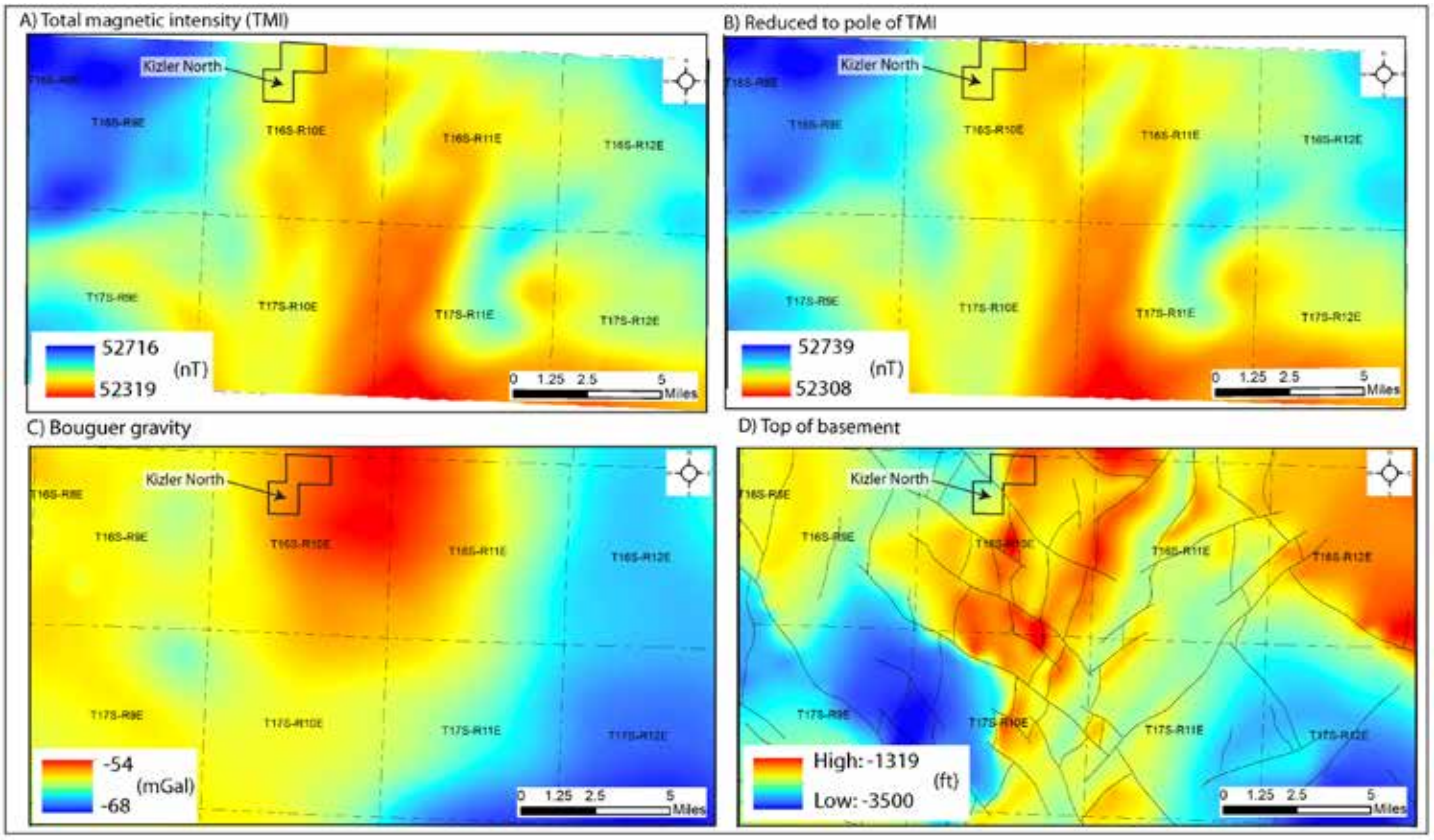

Figure 6. Potential fields dataset showing the basement architecture and faulting in the study area. Present-day sub-orthogonal fault blocks observed in the Precambrian basement likely result from episodes of strike-slip motion. (a) Total magnetic intensity (TMI) map, (b) reduced to pole map derived from TMI, (c) Bouguer gravity anomaly map, and (d) depth-to-basement surface map with major faults identified via Werner deconvolution. The black polygon indicates the approximate location of the Kizler North Field.

quantitative analyses were primarily based on a filtered magnetic field.

The basement structure map shows that the Precambrian basement of Kansas is dominated by conjugate NNE-SSW and NNW-SSE wrench fault blocks, with orthogonal to sub-orthogonal relationships (fig. 6d). At the basement high, the sediment thickness can be as little as 1,300 ft (~396 m), compared to 3,500 ft (~1,067 m) in thicker sedimentary sections (fig. 6d).

Seismic results

Five major secondary en echelon wrench faults (see f1–f5 in figs. 7–9) are present in the study area. Given similarities in time structure maps for the Precambrian basement (fig. 6d) and the Simpson, Viola, and "Hunton" groups (fig. 8b–d)—in addition to similarities in 2-D seismic (fig. 7)—these five faults appear to be sub-vertical, to terminate within or are pre-Chattanooga Shale in age (i.e., likely upper Devonian in age), and to cut through the Precambrian basement. The faults strike northwest, antithetical to the Nemaha anticline, one of the major subsurface structures in the region. Among the five Chattanooga to pre-Chattanooga wrench faults, three are visible within the Mississippian time structure map (fig. 8a, f2–f4) and can be observed within 2-D seismic extending into the overlying Pennsylvanian succession (fig. 7). The seismic lines show several dip direction changes for faults f3, f4, and f5 within the Mississippian and Pennsylvanian intervals (fig. 7). These faults exhibit probable flower structures, the centers of which appear downthrown with opposing fault dip directions to the S-SW or N-NE at angles of ~60° from horizontal and strike overall toward the northwest. In 2-D seismic (fig. 7), faults f3, f4, and f5 terminate either within the upper Kansas City-Lansing Groups' interval or lower Shawnee Group (i.e., Heebner Shale) interval. Of these three faults, fault f3 is the only fault that traverses seismic lines K2, K3, and K4 (see fig. 8a), indicating that this fault is more prominent and laterally extensive than faults f2 and f4. Lastly, the isochron map of the "Hunton Group" shows a W-NW thickening of this interval toward the axis of the Nemaha anticline and depocenter of the North Kansas basin (fig. 9).

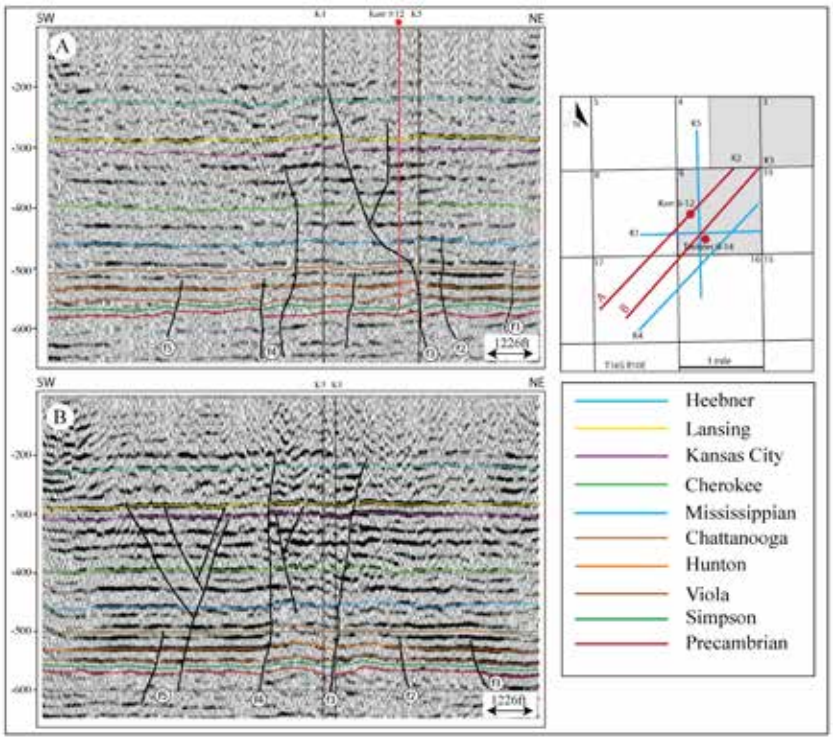

Figure 7. Detailed horizon and fault interpretation of seismic lines (a) K2 and (b) K3. Basement-rooted wrench faults are prominent in line K3. A flower structure, diagnostic of wrench systems, is observed in both seismic sections. Inset map shows location of the Kizler North Field (gray polygon) and seismic lines; horizon colors associated with stratigraphic tops are shown in the box on the lower right.

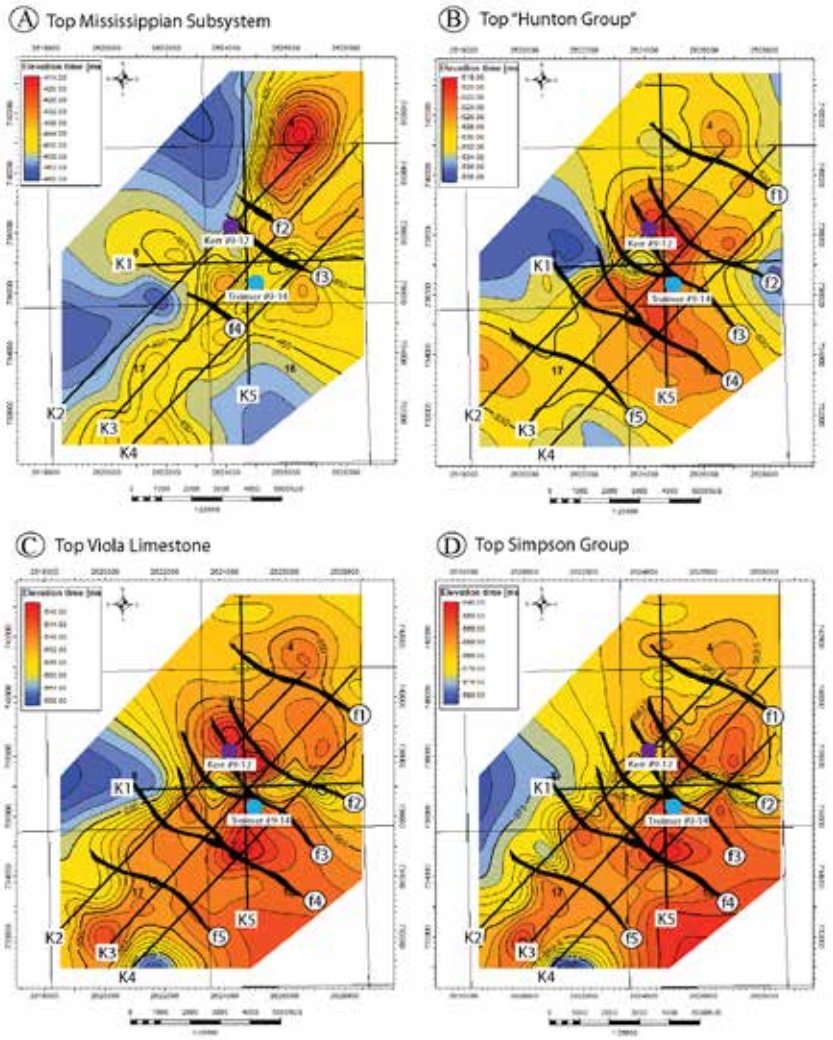

Figure 8. Kizler North Field time structure maps of key surfaces: (a) top Mississippian Subsystem, (b) top "Hunton Group," (c) top Viola Limestone, and (d) top Simpson Group. The maps show fewer and less extensive wrench faults in the Mississippian Subsystem compared to the pre-Mississippian horizons. Contour interval = 1 ms or approximately 6 ft. Locations of the seismic lines are shown in each map. Blue and violet dots represent the location of Treimer #9-14 and Kerr #9-12, respectively.

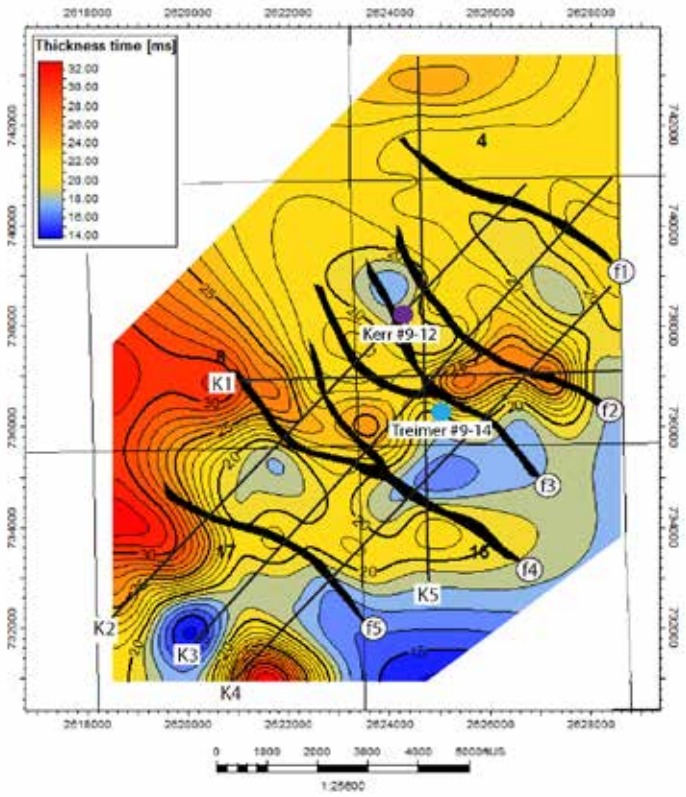

Figure 9. Kizler North 2-D "Hunton Group" isochron map (thickness in time). The "Hunton Group" is thin close to Kerr #9-12, where structure closure was observed in fig. 8b. Contour interval = 1 ms or approximately 6 ft. Blue and violet dots represent the location of Treimer #9-14 and Kerr #9-12, respectively.

Petrophysical results

The RHOMA-Umaa mineral composition cross-plot of the "Hunton Group" reservoir unit at the Treimer #9-14 well falls in the dolomite zone (fig. 5). Comparison of these data to petrophysical data collected at the Kerr #9-12, Treimer #14-2, and Treimer #9-14 wells indicates that the Simpson, Viola, and "Hunton" groups are dominantly dolomitic at all three well localities (fig. 10). Kerr #9-12 and Treimer #14-2 are observed to have higher water saturation than Treimer #9-14 (see Sw column in table 2) for all three units. The "Hunton Group" has 58.6% and 70.8% water saturation in the Kerr #9-12 and Treimer #14-2 wells, respectively, versus 48.6% at the Treimer #9-14 well. The Viola Limestone has 62.6% and 55.1% water saturation at the Treimer #14-2 and Kerr #9-12 wells, respectively, versus 49.8% at Treimer #9-14. Lastly, the Simpson Group, which could only be assessed at the Kerr #9-12 and Treimer #9-14 wells, has 55.6% and 30.5% water saturation, respectively. Total porosity (see PHIT column in table 2) varies minimally from 10% to 13% for all three reservoir units, whereas average clay volume (see Vcl column in table 2) ranges from 10% to 36% with the highest clay volume being observed in the "Hunton Group" at the Treimer #14-2 well.

Table 2. Petrophysical parameters from pay zone intervals within studied wells.

Zone	Top (ft)	Bottom (ft)	Gross (ft)	Net Res (ft)	PHIT	Sw	Vcl	Oil in place bbls (net res)
Well: TREIMER #9-14								
Hunton	2936.50	2977.50	41.00	11.50	0.129	0.486	0.209	64015
Viola	3044.00	3138.50	94.50	17.50	0.116	0.498	0.137	89760
Simpson	3138.50	3170.00	31.50	3	0.108	0.305	0.102	8774
Well: KERR #9-12								
Hunton	2996.50	3033.00	36.50	22.50	0.136	0.586	0.136	112204
Viola	3100.00	3194.00	93.50	23.00	0.119	0.551	0.067	94366
Simpson	3194.00	3223.00	29.00	3.50	0.105	0.556	0.231	12786
Well: TREIMER #14-2								
Hunton	3107.90	3163.90	56.00	4.75	0.116	0.708	0.359	Area of closure cannot be determined
Viola	3226.00	3321.00	95.00	5.50	0.119	0.626	0.099	
Simpson	No well log data to this depth							

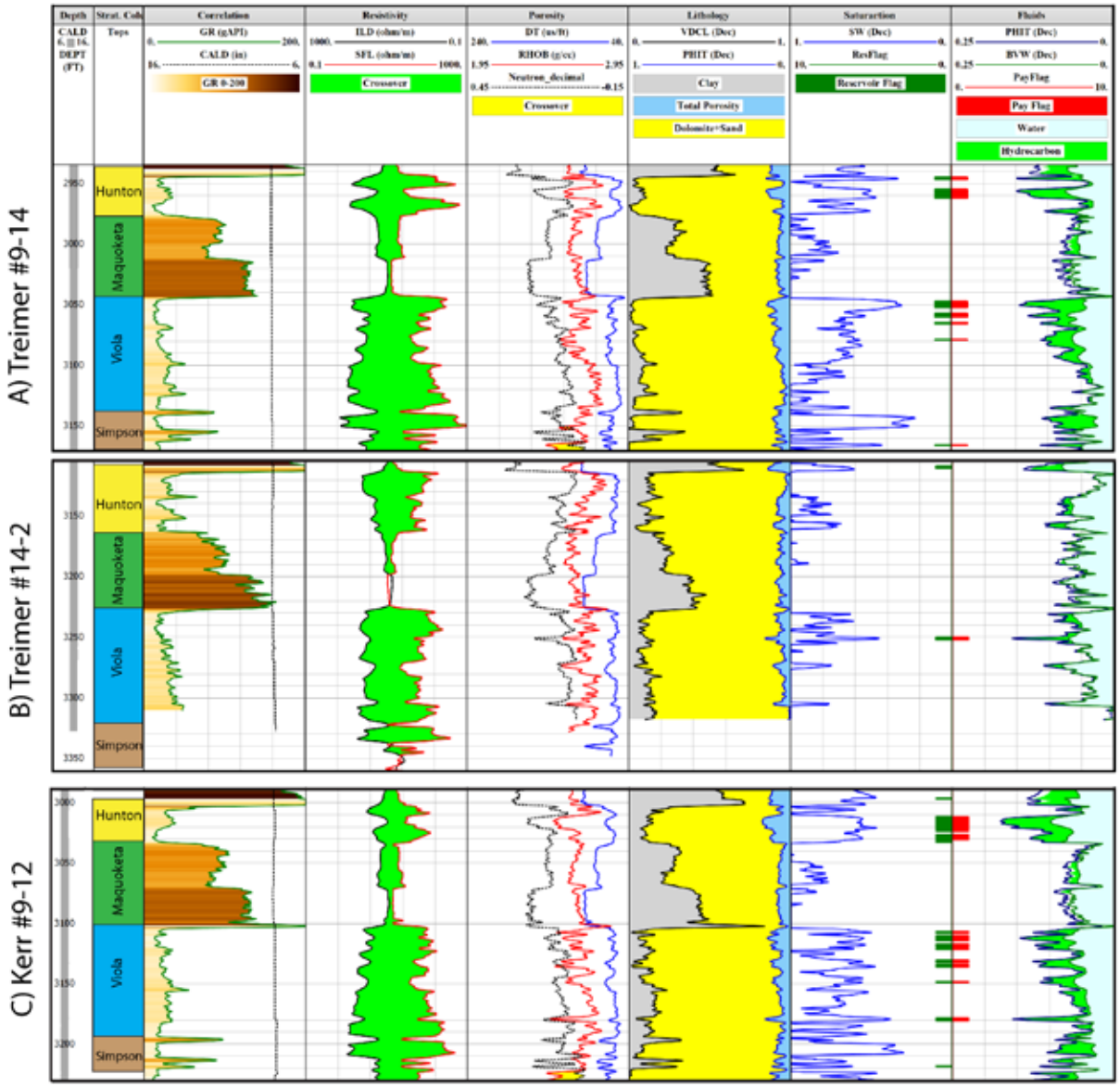

Figure 10. Petrophysical interpretation of the reservoir units: (a) Treimer #9-14, (b) Treimer #14-2, and (c) Kerr #9-12. Tracks one through five contain caliper (CALD), formation tops, gamma-ray (GR), resistivity (ILD = deep resistivity; SFL = shallow resistivity), and porosity (DT = sonic, RHOB = density, neutron_decimal = neutron) information, respectively. Track six contains lithology information where VDCL = volume of clay and PHIT = total porosity. Track seven contains water saturation values (SW) and reservoir flags. Lastly, track eight contains fluid and pay flag information (BVW = bulk volume of water).

DISCUSSION

Wrench faulting

Wrench faults (similarly used to define strike-slip faults) form in response to horizontal shear couples within Earth's crust where two adjacent blocks move sideways, horizontally, parallel to the strike of the fault zone (Wilcox et al., 1973; Mandl, 1988; Cunningham and Mann, 2007). The deformation mechanism of strike-slip faults simulated in clay models — by moving tin sheets beneath a clay cake — has been discussed extensively in previous literature (e.g., Jamison and Withjack, 1981; Mandl, 1988; and references therein). Such experiments have revealed the role of Riedel shear fractures (i.e., R-shear), which are a form of brittle deformation that accompanies strike-slip systems. These en echelon synthetic fractures (i.e., closely spaced and slip direction similar to main fault) propagate a short distance out from the main fault at an angle of roughly 15° to 20° (fig. 11; Sylvester, 1988). These Riedel shears are typically the first subsidiary fractures to develop (Swanson, 2006) and may be accompanied by associated secondary fractures. The two most prominent of these associated fractures are P shears (∠ 15° to 20° from main fault with opposing slip direction) and conjugate Riedel shears, or R′ shears (∠ 60° to 75° from main fault;

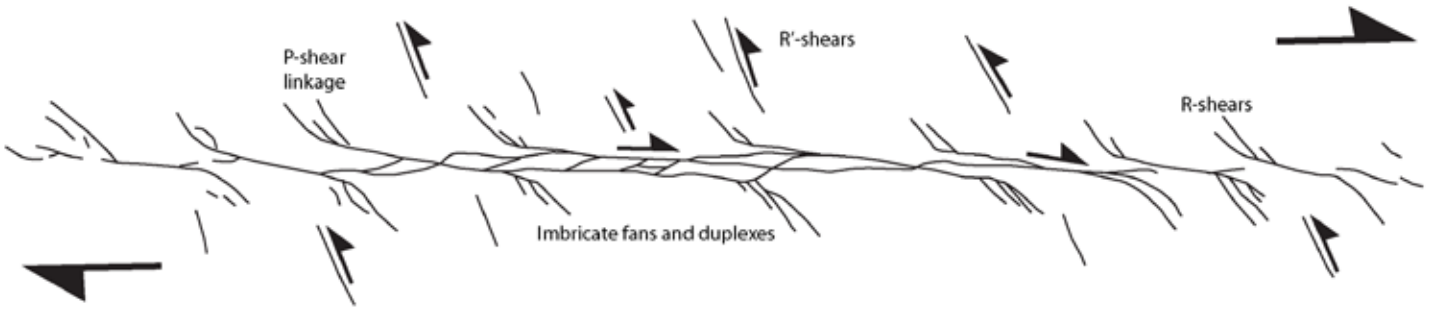

Figure 11. Fault zone terminology of Riedel shears along a strike-slip fault zone (modified from Swanson, 2006). The mapped faults from seismic sections are likely to be R-shear, P-shear, or R'-shear trends associated with wrenching of reactivated Precambrian basement faults. Slip appears very subtle, though there does appear to be offset in some structural blocks. The study area is small compared to the controlling regional tectonic elements.

Harding, 1985; Sylvester, 1988). These individual fractures remain active throughout the system's development so that synchronous movement on all fractures accommodates strain in the fault zone.

Our interpretation for the mapped faults being part of a wrench fault system are based on the following observations: a) presence of NNE-SSW and NNW-SSE orthogonal to sub-orthogonal crustal blocks, which were interpreted from potential fields data (fig. 6d), b) horizontal offsetting of the fault blocks in relation to each other (fig. 6d), c) change in the direction of dip ∠ of fault planes (fig. 7a and b), d) presence of flower structure in seismic sections (fig. 7b), and e) vertical to sub-vertical orientation of several fault planes and their extent to basement. The collective observation of these indicators, as described in Zalan (1987) and Harding (1990), led us to interpret them as being components of a larger wrench fault system. Though the slip signature is very subtle in seismic sections, and the study area is small compared to regional tectonic elements, the mapped faults from 2-D seismic sections are likely to be P-shear or R-shear trends of a regional basement wrench system (figs. 6d, 7, 8, 9). Similarly, given the high angle of NNE-SSW trending faults interpreted from potential fields data (fig. 6d) of greater than or equal to 60° from the main trend of faults observed in 2-D seismic (see figs. 7 and 8), it may be the case that a number of these faults are representative of conjugate Riedel shears associated with the main wrench system.

Effects from tectonics

A major change in the tectonic development of the Kansas region took place during post-Mississippian to pre-Desmoinesian time and defined much of the current structural framework of the Forest City basin (Merriam, 1963; Berendson and Blair, 1986). The cross-cutting relationships observed in our data show reactivation of pre-existing basement faults during this period (probably early Pennsylvanian). As the rigid basement complex is overlain by only a thin layer of sedimentary rocks, stresses transmitted through the basement in response to Phanerozoic orogenies would tend to deform the overlying rocks in a brittle manner (Berendsen and Blair, 1986).

The post-Mississippian to pre-Desmoinesian structural elements in Kansas show two sets of trends. The first is northeast (N20°E) aligned with the Nemaha anticline, and the second is northwest (N45°W) aligned with the coeval CKU (Merriam, 1963; Berendson and Blair, 1986). The identified wrench system in the Kizler North Field and accompanying secondary R, P, and R' structural elements suggest an overall northwest directional trend in the wrench fault system that aligns well with the CKU. The present structural elements of the CKU (see Cole, 1976) are considered to be closely related to structural elements that are Proterozoic in age (i.e., the ancestral CKU; Berendsen and Blair, 1986), which, based on interpretations by Baars (1995), became reactivated during the Ancestral Rocky Mountains Orogeny, resulting in northwesterly dextral displacement and uplift of the CKU. At that same time, northeasterly structural elements (e.g., Nemaha anticline) underwent a sense of sinistral displacement, thereby resulting in a transtensional stress regime along the MRS and Nemaha anticline. This stress is probably responsible for the wrench system and flower structures observed in the Kizler North Field (figs. 7–9). The basement structure map of the Kizler North Field (fig. 6d) shows that the Precambrian basement is dominated by conjugate NNE-SSW and NNW-SSE wrench fault blocks that exhibit orthogonal to sub-orthogonal relationships. We interpret these NNE-SSW and NNW-SSE trending structural elements to be sinistral and dextral strike-slip faults, respectively, an interpretation that is in alignment with the conclusions of Baars (1995).

Seismic data show that late-stage wrench faulting occurred during post-Mississippian to pre-Desmoinesian time (probably during the early Pennsylvanian). The timing of this wrenching event is evidenced by two key observations. First, the Mississippian time structure map shows altogether unique elevations in comparison to maps of the Simpson, Viola, and "Hunton" groups (fig. 8). Second, 2-D seismic clearly shows the reactivation of three lower Paleozoic fault traces — f3, f4, and f5 — that exhibit an abrupt shift in dip direction of ~60° within the Mississippian Subsystem and terminate within the Pennsylvanian succession (fig. 7). Given cross-cutting relationships and stratigraphic terminus of these faults within the upper Kansas City-Lansing Groups' interval or lower Shawnee Group (i.e., Heebner Shale) interval, we interpret this fault reactivation to be Pennsylvanian in age. The timing of this fault reactivation corresponds to documented reactivation of the CKU during the Ancestral Rocky Mountain Orogeny (Berendson and Blair, 1986); however, the wrenching implies reactivation of the MRS structural elements as well (e.g., Nemaha ridge), which created the documented sinistral offset.

The Pennsylvanian structural event resulted in a breach of the lower Paleozoic reservoirs and, in places, allowed for hydrocarbon migration out of the system (fig. 12). The wrench fault system at the Kizler North Field is an important trapping mechanism for petroleum accumulation. The study area contains two four-way dipping closures in the center of the map (subtle dome-like structures) terminated by adjacent wrench faults (fig. 8b, 8c).

Dry-hole analysis

Treimer #9-14 is the only producing well among the three studied wells, even though all of the wells have favorable reservoir qualities (e.g., high porosity and low clay volume) and four-way closure (KGS oil and gas wells database, 2020). The main difference between the producing Treimer #9-14 well and adjacent dry holes is water saturation. Treimer #14-2 shows significantly higher water saturation by as much as 22% than Treimer #9-14 (table 2). The water saturation in Kerr #9-12 is also approximately 10% higher than Treimer #9-14. The calculated oil in place in Kerr #9-12 is significant (as a function of the gross interval), but the operator deemed the well to be a dry hole because of high water saturation.

Though favorable reservoir qualities are present throughout the Kizler North Field, the structural nature of the area has resulted in high water saturation and lack of hydrocarbon accumulation. The dry hole (Treimer #14-2) directly overlies faults observed in the Mississippian surface map (fig. 8a). At this location, late-stage wrenching has breached the reservoir rocks and

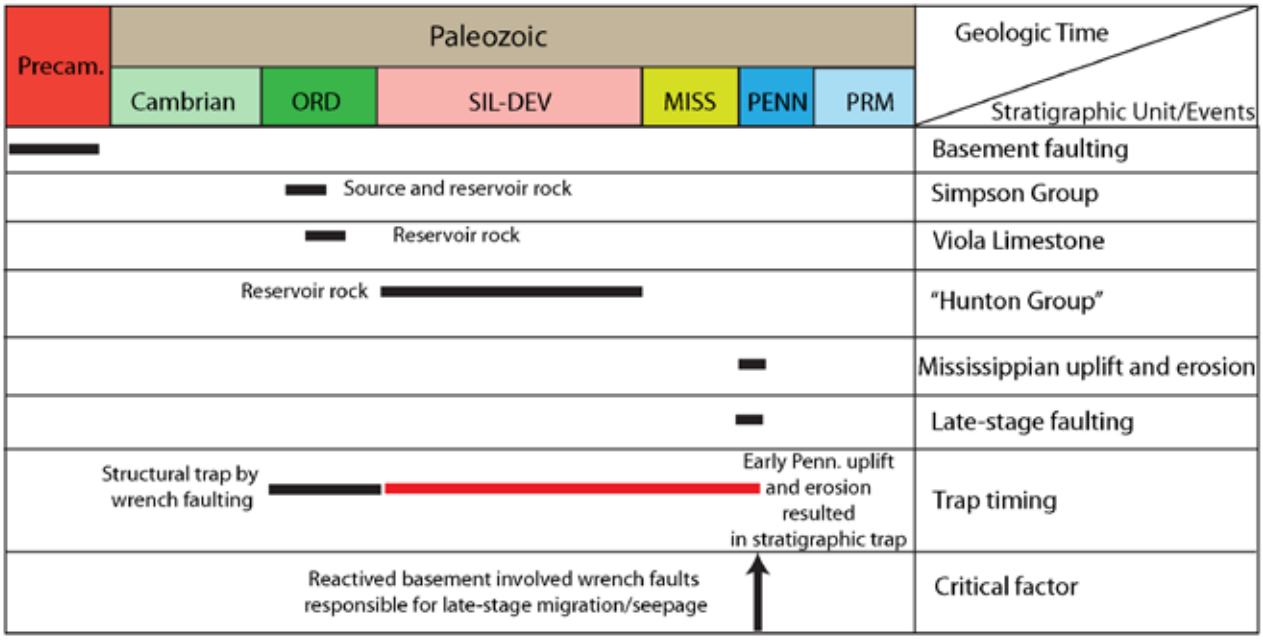

Figure 12. Event chart of petroleum systems of the Kizler North Field. The development of the Nemaha tectonic zone and Central Kansas uplift structural features are coeval (post-Mississippian to pre-Desmoinesian; Merriam, 2010). The timing of formation of the structural and stratigraphic traps are shown with black and red colored lines in the figure. The critical risk factor in this petroleum system is the reactivation of existing faults.

caused hydrocarbon migration out of the reservoirs (fig. 8a). An alternate explanation for high water saturation is that the reservoir was never charged due to the lack of maturation of the source rock. However, because these reservoirs are producing elsewhere in the same field, it is not likely that these reservoirs were never charged. The most likely explanation for the dry holes is that the post-Mississippian to pre-Desmoinesian reactivation of older faults and wrenching created migration pathways upward for hydrocarbons to leave the system and resulted in the higher water saturation observed in this well. Based on our interpretations, even if it is not economical to re-develop wells in this field, the play concept could be applied to similar basement-controlled structures within Kansas.

Play mechanism and exploration model

In summary, the source rock for the system is within the lower part of the Simpson Group (TOC greater than 1.1 wt% contains Type I and II kerogen; Jensik, 2013). The upper part of the Simpson Group and overlying Viola Limestone and "Hunton Group" act as the reservoir units and are predominantly dolomitic in composition with significant effective porosity (see figs. 5 and 10). The Mississippian rocks act, in part, as the sealing unit for these reservoirs, and it appears to be the case that late-stage reactivation of faults during post-Mississippian to pre-Desmoinesian time is responsible for the migration of hydrocarbons out of the reservoir. We observed a positive correlation between the locations of dry wells and well locations directly above reactivated faults. Our analysis indicates that the reservoir quality and charging do not differ much within the study area, and we suggest future exploration for analog fields should critically analyze the distribution of faults with structural closures.

CONCLUSION

The reactivation of basement faults during post-Mississippian to pre-Desmoinesian time resulted in the migration of petroleum out of some reservoirs. In the Kizler North Field as well as in analog fields where reactivated faults resulted in overprinting of structures by wrenching, it is crucial to look for faults that do not extend beyond the reservoir intervals. The dry well Kerr #9-12 is located directly on a structure that exhibits late-stage wrenching and propagation into the Pennsylvanian Subsystem. Even though the fault close to Treimer #9-14 does extend into the Pennsylvanian Subsystem, the associated reservoir is charged, likely because the well location is adjacent to the fault indicated in the Mississippian surface map and not directly over it (fig 8a). It is likely that the Simpson Group could produce from Treimer #9-14, as there is enough closure observed in the time structure map.

The exploration model for the Kizler North and analog fields is to look for subtle basement-rooted wrench fault systems that transect the reservoir dolomites with four-way closure. Future exploration models for analog fields should be based on the following criteria: 1) four-way closure with wrench-fault-related traps, 2) structural closures in the Viola Limestone and Simpson Group, 3) thick "Hunton Group," and 4) presence of a wrench fault that creates subtle closure adjacent to the well location but not directly beneath it.

ACKNOWLEDGMENTS

The authors are grateful to Running Foxes Petroleum Inc. for providing the dataset for this study. Gratitude is extended to Schlumberger for the donation of Petrel software and Lloyd's Register for Interactive Petrophysics software (both to Potter-McIntyre). The authors would also like to thank Bill Cathey and Earthfield Technology for their contribution to the Werner deconvolution of aeromagnetic data. We appreciate the constructive comments of Stephan Oborny, Franek Hasiuk, and an anonymous reviewer that improved this paper.

REFERENCES CITED

Archie, G. E., 1952, Classification of carbonate reservoir rocks and petrophysical considerations: AAPG Bulletin, v. 36, no. 2, p. 278–298. https://doi.org/10.1306/3D9343F7-16B1-11D7-8645000102C1865D

Baars, D. L., 1995, Basement tectonic configuration in Kansas; in, Geophysical Atlas of Selected Oil and Gas Fields in Kansas, N. L. Anderson and D. E. Hedke, eds.: Kansas Geological Survey and Kansas Geological Society, Bulletin 237, p. 7–9.

Baker, D. R., 1962, Organic geochemistry of the Cherokee Group in southeastern Kansas and northeastern Oklahoma: AAPG Bulletin, v. 46, p. 1,621–1,642. https://doi.org/10.1306/BC7438D9-16BE-11D7-8645000102C1865D

Berendsen, P., and Blair, K. P., 1986, Subsurface structural maps over the Central North American Rift System (CNARS), central Kansas, with discussion: Kansas Geological Survey Subsurface Geology Series, v. 8, 16 p., 7 sheets, scale: 1:250,000.

Brooks, L., and Montalvo, R., 2012, The integration of key petrophysical and geomechanical play drivers into geologic attribute mapping: Getting ahead of the stampede: AAPG Search and Discovery, v. 40948, p. 79.

Burberry, C. M., Joeckel, R. M., and Korus, J. T., 2015, Post-Mississippian tectonic evolution of the Nemaha Tectonic Zone and Midcontinent Rift System, SE Nebraska and N Kansas: Papers in the Earth and Atmospheric Sciences, p. 461.

Cansler, J. R., and Carr, T. R., 2001, Paleogeomorphology of the Sub-Pennsylvanian unconformity of the Arbuckle Group (Cambrian-Lower Ordovician): Kansas Geological Survey Open-File Report 2001-55, 2 sheets.

Carlson, M. P., 1999, Transcontinental Arch — A pattern formed by rejuvenation of local features across central North America: Tectonophysics, v. 305, p. 225–233. https://doi.org/10.1016/S0040-1951(99)00005-0

Choquette, P. W., and Pray, L. C., 1970, Geological nomenclature and classification of porosity in sedimentary carbonates: AAPG Bulletin, v. 54, p. 207–250.

Cole, V. B., 1976, Configuration of the top of the Precambrian rocks in Kansas: Kansas Geological Survey, Map M-7, 1 sheet, 1:500,000.

Cunningham, W. D., and Mann, P., 2007, Tectonics of strike-slip restraining and releasing bends: Geological Society of London, Special Publications, 290, p. 1–12. https://doi.org/10.1144/SP290.1

Gerhard, L. C., 2004, A new look at an old petroleum province: Current Research in Earth Sciences, Kansas Geological Survey, Bulletin 250, part 1, 27 p. http://www.kgs.ku.edu/Current/2004/Gerhard/index.html

Harding, T. P., 1985, Seismic characteristics and identification of negative flower structures, positive flower structures and positive structural inversion: AAPG Bulletin, v. 69, no. 4, p. 582–600. https://doi.org/10.1306/AD462538-16F7-11D7-8645000102C1865D

Harding, T. P., 1990, Identification of wrench faults using subsurface structural data: Criteria and pitfalls: AAPG Bulletin, v. 74, no. 10, p. 1,590–1,609.

Hasan, M. N., 2019, Reservoir characterization of the Kizler North Field, Lyon Co., Kansas, USA: unpublished M.S. thesis, Southern Illinois University (Carbondale), 120 p.

Jamison, W. R., and Withjack, M. O., 1981, Clay model experiments of fault patterns produced by combined wrenching and rifting: EOS, v. 62, p. 1,032.

Jensik, C., 2013, Geologic controls on reservoir quality of the Viola Limestone in Soldier Field, Jackson County, Kansas: unpublished M.S. thesis, Kansas State University, 41 p.

Kansas Geological Survey, 2020, Oil and gas wells database. http://www.kgs.ku.edu/Magellan/Qualified/

Ku, C. C., and Sharp, J. A., 1983, Werner deconvolution for automated magnetic interpretation and its refinement using Marquardt inverse modeling: Geophysics, v. 48, p. 754–774. https://doi.org/10.1190/1.1441505

Lee, W., 1943, The stratigraphy and structural development of the Forest City basin in Kansas: Kansas Geological Survey, Bulletin 51, p. 142.

Mandl, G., 1988, Mechanics of Tectonic Faulting: Models and Basic Concepts; Developments in Structural Geology Vol. 1, H. J. Zwart, series ed.: Amsterdam, Elsevier, 407 p.

Merriam, D. F., 1963, The geologic history of Kansas: Kansas Geological Survey Bulletin 162, 317 p..

Merriam, D. F., 2010, The geology and petroleum resources of Kansas: A review from alpha to omega or from the Pleistocene to the Precambrian: Natural Resources Research, v. 19, p. 293–316. https://doi.org/10.1007/s11053-010-9125-x

Merriam, D. F., and Goebel, E. D., 1956, Kansas structural provinces offer varied types of traps: Oil and Gas Journal, v. 54, no. 52, p. 141–154.

O'Connor, H. G., 1953, Geology, mineral resources, and ground-water resources of Lyon County, Kansas: Kansas Geological Survey, Volume 12, 59 p. http://www.kgs.ku.edu/General/Geology/Lyon/index.html

Onajite, E., 2014, Seismic Data Analysis Techniques in Hydrocarbon Exploration: Amsterdam, Elsevier, 256 p. https://doi.org/10.1016/C2013-0-09969-0

Sims, P. K., 1990, Precambrian basement map of the northern midcontinent, U.S.A.: U.S. Geological Survey, Map I-1853-A.

Swanson, M. T., 2006, Late Paleozoic strike-slip faults and related vein arrays of Cape Elizabeth, Maine: Journal of Structural Geology, v. 28, no. 3, p. 456–473. https://doi:10.1016/j.jsg.2005.12.009

Sylvester, A. G, 1988, Strike-slip faults: Geological Society of America Bulletin, v. 100, no. 11, p. 1,666–1,703. https://doi.org/10.1130/0016-7606(1988)100%3C1666:SSF%3E2.3.CO;2

Tedesco, S., 2015, The cause of gas saturation in the coals of the Cherokee Formation (Desmoinesian Age) in the Cherokee and Forest City basins, Mid-Continent, USA: AAPG Search and Discovery Article #80490. https://www.searchanddiscovery.com/documents/2015/80490tedesco/ndx_tedesco.pdf

Tedesco, S., 2017, Identification of petroleum productive low temperature hydrothermal dolomite reservoirs: Difficulties and challenges identifying and finding: AAPG Search and Discovery Article #42039. https://www.searchanddiscovery.com/documents/2017/42039tedesco/ndx_tedesco.pdf

Van Schmus, W. R., Bickford, M. E., Sims, P. K., Anderson, R. R., Shearer, C. K., and Treves, S. B., 1993, Proterozoic geology of the western midcontinent basement; in, Precambrian: Conterminous U. S., J. C. Reed, Jr., M. E, Bickford, R. S. Houston, P. K. Link, D. W. Rankin, P. K. Sims, and W. R. Van Schmus, eds.: Geological Society of America, v. C-2, p. 239–259.

Werner, S., 1953, Interpretation of magnetic anomalies at sheet-like bodies: Sveriges Geologiska Undersokning. Series C, Arsbok, 6, p. 413-449.

Wilcox R. E, Harding T. T, and Seely D. R., 1973, Basic wrench tectonics: AAPG Bulletin, v. 57, no. 1, p. 74–96. https://doi.org/10.1306/819A424A-16C5-11D7-8645000102C1865D

Zalan, P. D., 1987, Identification of strike-slip faults in seismic sections: SEG Technical Program Expanded Abstracts, p. 116–118. https://doi.org/10.1190/1.1892142

Zeller, D. E., ed., 1968, The stratigraphic succession in Kansas: Kansas Geological Survey, Bulletin 189, 81 p., 1 plate.

Midcontinent Geoscience • Volume 2 • May 2021
Tony Layzell – Editor
Section Editor — Franek Hasiuk
Technical Editor — Julie Tollefson

Suggested citation: Hasan, M. N., Potter-McIntyre, S., and Tedesco, S., 2021, Wrench faulting and trap breaching: A case study of the Kizler North Field, Lyon County, Kansas, USA: Midcontinent Geoscience, v. 2, p. 1–14.

Midcontinent Geoscience is an open-access, peer-reviewed journal of the Kansas Geological Survey. The journal publishes original research on a broad array of geoscience topics, with an emphasis on the midcontinent region of the United States, including the Great Plains and Central Lowland provinces.

Submission information: https://journals.ku.edu/mg/about/submissions

Kansas Geological Survey
1930 Constant Avenue
The University of Kansas
Lawrence, KS 66047-3724
785.864.3965

http://www.kgs.ku.edu/

KU
KANSAS
GEOLOGICAL
SURVEY
The University of Kansas